Water Practice & Technology

IWA PUBLISHING



Water Practice & Technology Vol 18 No 7, 1663 doi: 10.2166/wpt.2023.103

# Bioaugmentation of a structural extracellular polymeric substances (EPS) producer to improve activated sludge bioflocculation: lessons learned

An-Sofie Christiaens [a], Robin Daenen[b] and Ilse Smets [a,*]

[a] Chemical and Biochemical Reactor Engineering and Safety (CREaS), Chemical Engineering Department, KU Leuven, Celestijnenlaan 200f box 2424, 3001 Heverlee, Belgium
[b] Center for Microbial Ecology and Technology (CMET), Faculty of Bioscience Engineering, Ghent University, Coupure Links 653, 9000 Gent, Belgium
*Corresponding author. E-mail: ilse.smets@kuleuven.be

A-SC, 0000-0002-5751-1990; IS, 0000-0001-8570-5568

## ABSTRACT

Structural extracellular polymeric substances (EPS) contribute to the bioflocculation performance of activated sludge systems. This research investigates the potential of bioaugmentation of a structural EPS producer, *Azoarcus communis*, as a bioflocculation improvement or remediation approach. An antibiotic-resistant and fluorescent protein-producing mutant was constructed to monitor the survival, persistence, and location of the augmented strain in the membrane bioreactor. Preliminary batch tests against a kaolin clay model system and deflocculated sludge revealed the flocculation potential of this strain. Morphological image analysis and fluorescence microscopy suggest that most of the bacteria augmented in suspension were initially attached to the sludge flocs with, however, only a limited fraction getting incorporated within the activated sludge floc biomass. This limited bioaugmentation prevented assessing its impact on bioflocculation and might be explained by metazoan and protozoan grazing, together with competition with indigenous organisms and sub-optimal growth conditions in the reactor for the engineered strain.

**Key words:** amyloid adhesins, biological wastewater treatment, flocculation activity, fluorescent protein

## HIGHLIGHTS

- The structural EPS producer *Azoarcus* is bioaugmented to enhance sludge bioflocculation.
- Augmentation with an antibiotic-resistant and fluorescent mutant strain ensures proper enumeration and localization.
- *Azoarcus* initially attached to sludge flocs but long-term persistence was limited.
- An MBR setup avoids initial washout but grazing by metazoa and protozoa remains a problem.

## GRAPHICAL ABSTRACT

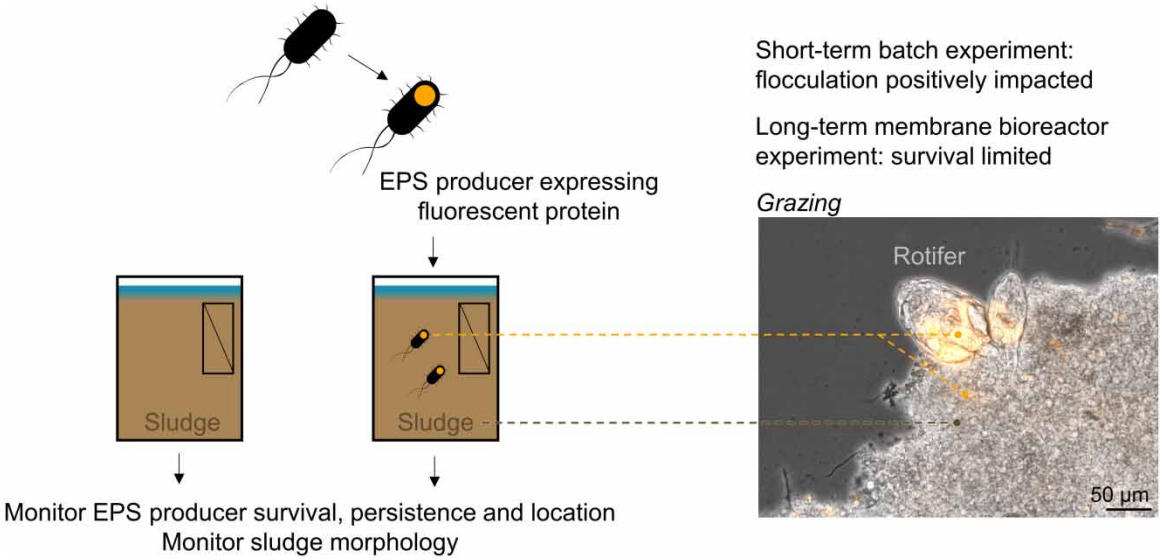


## 1. INTRODUCTION

Bioaugmentation or the addition of indigenous or allochthonous wild-type or genetically modified organisms is used to solve practical problems in several biotechnological domains. This technique is often aimed at improving the catabolism of specific compounds in wastewater treatment plants. To a lesser extent, it has been exploited to enhance the bioflocculation performance of microorganisms. An evident example is the seeding of granules or biofilms, as summarized in a review within the context of accelerating aerobic granule formation or improving granule stability (Kent *et al.* 2018). A more targeted approach is described by Xin *et al.* (2017), who augmented a *Rhodocyclaceae*-related *Acinetobacter* sp. named TN-14 with heterotrophic nitrification and aerobic denitrification function, which promoted aerobic granule development. This strain promoted the EPS production of sludge, by increasing the hydrophobicity. Similarly, the harvesting efficiency of microalgae has been improved by mixing them with cultures of bacteria, fungi, or flocculating strains of microalgae (Demir *et al.* 2020) producing extracellular polymers. The latter review also describes cases where the extracellular polymers are extracted and added as bioflocculants to the microalgae culture. In a similar context, Sarang & Nerurkar (2020) use a bioflocculant extracted from *Bacillus cereus* CR4 for application in microalgae harvesting. Congo red and Thioflavin T (ThT) staining of the bacterial culture and other assays, including transmission electron microscopy and Fourier-transform infrared spectroscopy, on the purified extract identified the bioflocculant as an amyloid adhesin. Amyloid adhesins are highly stable proteinaceous molecules that are part of the structural EPS and are previously investigated by our research group (Christiaens *et al.* 2022) and other groups.

These studies suggest a potential for augmentation of pure cultures, specifically structural EPS producers, as targeted bioflocculation remediation approaches within the field of wastewater treatment.

This potential will be investigated in this work using *Azoarcus*, which was identified as a promising candidate for this augmentation experiment based on the following characteristics. *Azoarcus* are chemoorganoheterotrophs that can use $O_2$ or $NO_3^-$ as an electron acceptor. *Azoarcus* species are believed to be one of the dominant denitrifiers in intermittently aerated nitrifying and denitrifying sludge from plants treating industrial and coking wastewater (Juretschko *et al.* 2002; Ma *et al.* 2015) as well as in communal wastewater treatment plants with biological nitrogen and phosphorus removal (Thomsen *et al.* 2007). Recent data from 368 plants with relevant process types (carbon and nitrogen removal with or without enhanced biological phosphorus removal) reports a global maximum of 1.4% relative abundance (Dueholm *et al.* 2022). *Azoarcus* belong to the phylogenetic group of Betaproteobacteria that are known to be strong microcolony formers with high resistance to shear stress (Klausen *et al.* 2004). *Azoarcus* belong to the family of *Rhodocyclaceae* in which many EPS-producing denitrifiers are classified (Rosenberg *et al.* 2014). More specifically, an extracellular polysaccharide biosynthesis gene cluster similar to the one in *Zoogloea* and linked to floc formation in *Azoarcus* has been identified (An *et al.* 2016). Moreover, *Azoarcus* has been identified as a potential amyloid producer based on sequential ThT staining

and fluorescence *in situ* hybridization, but these results were not confirmed with conformational antibodies (Larsen *et al.* 2008).

This study aims to further explore the impact of structural EPS producers on bioflocculation in general and on bioaugmentation of *Azoarcus communis* in particular. Three research hypotheses were formulated: (*i*) *A. communis* is a bioflocculation-stimulating activated sludge organism, (*ii*) more amyloid-like substances can be introduced to activated sludge via augmentation of *A. communis*, and (*iii*) bioflocculation of activated sludge can be improved via augmentation of *A. communis*. In order to enable targeted monitoring of the survival, persistence, and incorporation of the augmented structural EPS producer, this study constructed an antibiotic-resistant and fluorescent mutant strain.

## 2. MATERIALS AND METHODS

### 2.1. Organisms and culture conditions

A freeze-dried culture of *A. communis* Swub 3 (DSM12120) was acquired from the Deutsche Sammlung von Mikroorganismen (DSMZ) databank. An *Escherichia coli* K-12 curli-deficient mutant (SM2257) (Prigent-Combaret *et al.* 2001) and a mutant with upregulated curli production (SM5578) (Vidal *et al.* 1998) were used as model organisms. All strains were cultured aerobically at 28 °C. *A. communis* was grown overnight after inoculation at an initial optical density ($OD_{600}$) of 0.05 in shake flasks in tryptic soy broth (TSB) consisting of 17 g $L^{-1}$ pancreatic digest of casein, 3 g $L^{-1}$ papaic digest of soybean 3 g $L^{-1}$, 2.5 g $L^{-1}$ glucose, 5 g $L^{-1}$ NaCl, 2.5 g $L^{-1}$ $K_2HPO_4$. *E. coli* SM2257 and SM2258 were grown statically for 48 h after inoculation at an initial $OD_{600}$ of 0.05 in the M63 medium (Larsen *et al.* 2007).

### 2.2. Construction of rifampicin-resistant and fluorescent *A. communis* mutants

Rifampicin powder (Sigma–Aldrich) was dissolved in DMSO and filter sterilized through a 0.2-μm syringe filter. The concentration of the stock solution was determined spectrophotometrically by absorbance measurement at 475 nm. From this absorbance, the concentration was calculated via the Lambert–Beer law with the molar extinction coefficient equal to 15,400 $M^{-1}$ $cm^{-1}$ for rifampicin in phosphate buffer (Florey 1976). A gentamicin sulfate sterile filtered 50 mg $mL^{-1}$ solution in water was purchased from Merck Life Science.

Rifampicin-resistant ($Rif^r$) mutants were constructed by inoculation of the *A. communis* bacterial stock onto tryptic soy agar (TSA) plates supplemented with 50 mg $L^{-1}$ rifampicin. Spontaneous rifampicin-resistant mutants were replated three times to TSA containing 100 mg $L^{-1}$ rifampicin. Finally, colonies from these plates were grown overnight at 28 °C in TSB supplemented with 100 mg $L^{-1}$ rifampicin, harvested by centrifugation at 3,220 *g* for 10 min, and stored in 20% w/v glycerol at −80 °C in sterile cryovials until further use.

Fluorescent-labeled bacteria were constructed using the mini-Tn5 random transposon insertion system as described first by De Lorenzo *et al.* (1990). Briefly, a minitransposon delivers the plasmid, containing a fluorescent protein gene and an antibiotic resistance gene as a selection marker, from a donor strain to a host strain. The *E. coli* S17-I λpir::pMRE-Tn5-145 donor strain, conferring gentamicin resistance and mScarlet-I encoding for red-fluorescent proteins, was grown for 6 h at 37 °C until the exponential growth phase in lysogeny broth (LB) consisting of 10 g $L^{-1}$ tryptone, 5 g $L^{-1}$ yeast extract, and 10 g $L^{-1}$ NaCl, supplemented with 20 mg $L^{-1}$ gentamicin. The *A. communis* $Rif^r$ host strain was grown overnight at 28 °C until the early stationary phase in TSB supplemented with 100 mg $L^{-1}$ rifampicin. Cells were harvested by centrifuging 5 mL of culture for 10 min at 3,220 g, washed three times using sterile 0.9% NaCl to remove all antibiotics, and resuspended in 500 μL 0.9% NaCl to obtain a dense suspension. Bi-parental mating was performed by spotting 20 μL of a 1:1 donor:host mix on a TSA plate. After 24 h of incubation at 28 °C, cells were scraped off, suspended in 0.9% NaCl, and plated on TSA supplemented with 100 mg $L^{-1}$ rifampicin and 20 mg $L^{-1}$ gentamicin to select for transconjugants. Fluorescent mutants were identified using a Safe Imager™ 2.0 Blue-Light Transilluminator, grown in TSB supplemented with 100 mg $L^{-1}$ rifampicin and 20 mg $L^{-1}$ gentamicin, harvested, and stored in 20% w/v glycerol at −80 °C in sterile cryovials until further use. The *A. communis* mutant carrying the mScarlet-I gene is hereafter referred to as *A. communis* $Rif^r$-mSc.

The identity of the fluorescent mutant strain was checked via Sanger sequencing. Cells were picked from the agar plate and suspended in UV-sterilized nuclease-free water and lysed at 95 °C for 5 min (Horecka & Chu 2017). The partial 16S rRNA genes were amplified using the universal primer pair 27F (5′-AGA–GTT–TGA–TCM–TGG–CTC–AG-3′) and 1492R (5′-GGT–TAC–CTT–GTT–ACG–ACT–T-3′) (Frank *et al.* 2008) using the PCR conditions described in Supplementary material S1. The amplicon was purified from primers, primer

dimers, and deoxynucleotide triphosphates (dNTPs) using the QIAquick PCR Purification kit (QIAGEN®) according to the manufacturer's instructions. Sanger sequencing was performed by GATC Biotech AG, Germany. The resulting partial 16S rRNA gene sequences were aligned with NCBIs refseq_rna databased for Reference RNA sequences using the MegaBLAST program optimized for highly similar sequences in BLASTN version 2.13.0+ (Altschul *et al.* 1990; Zhang *et al.* 2000).

To check whether the inserted mutations affected growth, the growth rate of the wild-type and mutant strains was determined. Replicate cultures were inoculated at an initial $OD_{600}$ of 0.05, and their $OD_{600}$ was measured at specific time intervals as a proxy for cell density. Based on these data, the specific growth rate $\mu$ was estimated by multi-phase linear regression using MATLAB® R2022b (MathWorks®) as detailed in Supplementary material S2.

To check the stability of the insertion of the antibiotic and fluorescent markers, the mutant was grown overnight at 28 °C and 150 rpm in TSB containing 100 mg $L^{-1}$ rifampicin and 20 mg $L^{-1}$ gentamicin. The culture was washed 3 times in 0.9% NaCl to remove all antibiotics prior to dilution to an $OD_{600}$ of 0.05. A subculture was inoculated by transferring 50 µL of this culture into 25 mL fresh TSB without antibiotics and grown until the late exponential phase at 28 °C and 150 rpm for around 24 h. This procedure was followed by 10 successive similar transfers. Finally, the colony-forming units CFU method was used to quantify the stability of the antibiotic markers: a series of tenfold dilutions was prepared in a 96-well plate. Six 5 µL replicates were spotted on rectangular TSA plates with and without the antibiotics rifampicin and gentamicin, and the antifungal additive nystatin (Thermo Scientific™). A 5 mg $mL^{-1}$ stock solution of nystatin in DMSO was prepared. Plates were incubated for a minimum of 48 h at 28 °C before counting. Experimental data were analyzed for statistical significance using a Student's *t*-test using MS Excel. Additionally, 20 colonies were picked and dissolved in PBS, and their fluorescence was assessed under the Olympus IX83 fluorescence microscope.

### 2.3. Characterization of *A. communis*: amyloid production and flocculation activity index

Amyloid-like substances were detected and the ThT emission signal was quantified as described before (Christiaens *et al.* 2022). Prior to ThT staining, cultures were grown in TSB were washed twice using PBS to remove the autofluorescent growth medium.

The bioflocculation activity of the *A. communis* $Rif^r$-mSc mutant was estimated against two suspensions as visualized in Figure 1. A kaolin clay suspension (Merck) is typically used for this purpose and was proposed by Kurane *et al.* (1986) as a reproducible yet oversimplified model system. The colloidal kaolin clay particles are negatively charged at alkaline pH leading to electrostatic repulsion between them (Dwari & Mishra 2019 and references therein). A (bio)flocculant might precipitate the kaolin particles by charge neutralization, cation-mediated bridging, or direct attachment and bridging (Liu *et al.* 2015). Quantification of the bioflocculation activity was roughly based on the method by Liu *et al.* (2010). Briefly, kaolin or sludge and *Azoarcus* in PBS were added to a final volume of 10 mL and a final concentration of 1 g $L^{-1}$ each, each in a 15 mL Greiner tube. The sample was stirred in a head-over-end mixer for 2 min. After 5 min of settling, 1 mL was carefully pipetted from the top and analyzed spectrophotometrically. Deflocculation and settling steps were performed on ice to avoid the reflocculation of the activated sludge. Typically, the flocculation activity index (FAI) is calculated according to Equation (1) with $A_{550}$ the absorbance at 550 nm, *kb* the clarifying suspension of kaolin and bioflocculant, and *k* the kaolin-only control. This equation is only correct when the bioflocculant is extracted and separated from the producer cells. In this experiment, however, the suspended biomass contributed to the total

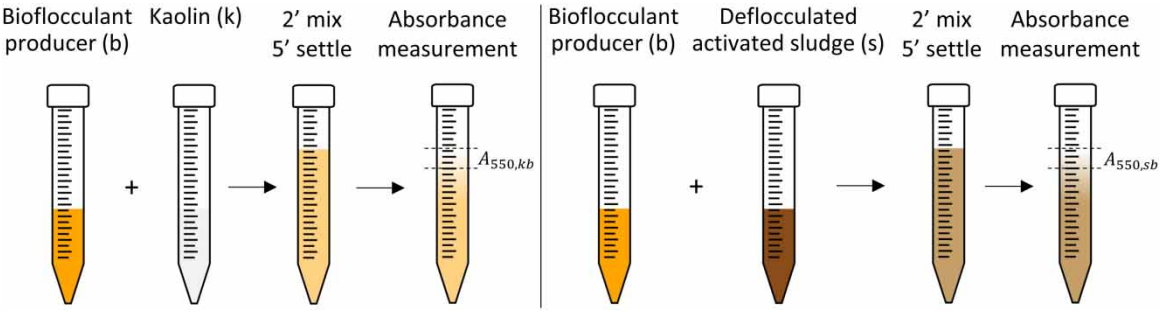


**Figure 1** | Graphical representation of the experimental approach followed to quantify the bioflocculation activity against kaolin clay (left) and deflocculated sludge (right).

absorbance. This bias is corrected for in Equation (2) with $b$ the control without kaolin. Results were compared with the *E. coli* SM2257 curli-deficient mutant and SM2258 mutant with upregulated curli production as replacers of *Azoarcus*. The experiment was repeated against activated sludge after deflocculation with a UP50H ultrasound horn and MS7 sonotrode (Hielscher) operated at 50 W with an amplitude of 75% for 2 min, and the corresponding FAI is calculated according to Equation (3) with $s$ the deflocculated activated sludge.

$$\text{FAI } [\%] = \frac{A_{550,k} - A_{550,kb}}{A_{550,k}} \times 100\% \tag{1}$$

$$\text{FAI } [\%] = \frac{A_{550,k} + A_{550,b} - A_{550,kb}}{A_{550,k} + A_{550,b}} \times 100\% \tag{2}$$

$$\text{FAI } [\%] = \frac{A_{550,s} + A_{550,b} - A_{550,sb}}{A_{550,s} + A_{550,b}} \times 100\% \tag{3}$$

### 2.4. Parallel membrane bioreactor setup and operation

A schematic of the used laboratory-scale membrane bioreactor (MBR) setup is presented in Figure 2. The reactor setup described before (Christiaens *et al.* 2022) was retrofitted with an ultrafiltration membrane for the bioaugmentation experiment. Membranes were fabricated similar to the method described by Marbelia *et al.* (2019) but starting from a 15 wt% polyvinylidene fluoride (PVDF, 534 kDa, Sigma–Aldrich)) and 5 wt% poly(vinylpyrrolidone) (PVP, 10 kDa, Sigma–Aldrich, Belgium) in dimethylformamide (DMF, >99.9% pure, Acros Organics, Belgium) polymer solution. Briefly, flat sheet membranes were prepared via phase inversion using an automated casting machine (Agila NV, Belgium) resulting in an estimated average pore size of 1 μm. To assemble the membrane module, flat sheets were folded around a flat woven spacer and glued in between a frame using epoxy-based glue (UHU) to weigh down and avoid floating. The resulting membrane module had an active filtration surface of 0.0132 $m^2$. A WIKA model DG-10 digital pressure gauge measured the transmembrane pressure (TMP).

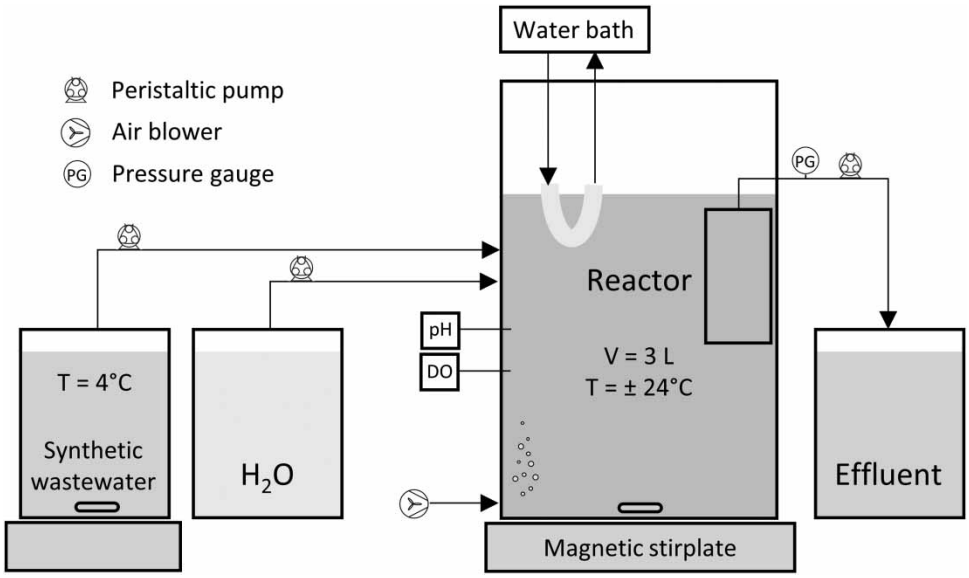


**Figure 2** | Schematic representation of the laboratory-scale MBR setup.

Membranes were regularly cleaned chemically using 2% sodium hypochlorite to keep the TMP under 500 mbar. HRT and SRT were kept constant at 48 h and 20 days, respectively. The 144-min reaction cycle, represented schematically in Figure 3, consisted of an anoxic (60 min) and aerobic phase (84 min). Permeate was withdrawn during the aerated phase in 10-min intervals followed by a 1-min membrane relaxation phase during which the cake layer could be scoured off. The reactors were fed with synthetic wastewater adapted from (Van den Broeck *et al.* 2010) with a composition of 85:6:1 COD:N:P. and a ratio of monovalent to

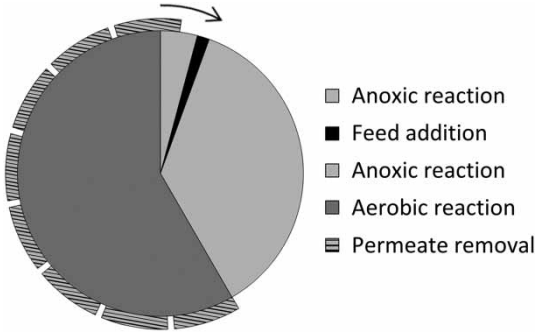


**Figure 3** | Schematic representation of the operational cycles of the laboratory-scale MBR setup. Total cycle time: 144 min.

polyvalent cations of 1.83 and consisted of 203 mg $L^{-1}$ $(CH_3COO)_2Ca.H_2O$, 483 mg $L^{-1}$ $CH_3COONH_4.H_2O$, 895 mg $L^{-1}$ $C_6H_{12}O_6$, 95.3 mg $L^{-1}$ yeast extract, 78.5 mg $L^{-1}$ $(NH_4)_2HPO_4$, 45.0 mg $L^{-1}$ KCl, 69.6 mg $L^{-1}$ $Na_2SO_4$, 188 mg $L^{-1}$ $MgCl_2{\cdot}6H_2O$, 57.5 mg $L^{-1}$ $CaCl_2{\cdot}2H_2O$, and 9.11 mg $L^{-1}$ $FeCl_3$. Sludge morphology was monitored using an Olympus IX83 inverted microscope with cellSens Dimension software and an in-house developed MATLAB® based image analysis software (Jenné *et al.* 2007).

The inoculum was obtained from a full-scale aerobic municipal wastewater treatment plant operated by Aquafin (Leuven, Belgium) on February 2, 2022. Prior to augmentation, the parallel reactors were operated for 40 days to allow the microbial community to adapt to the changed environment. After this startup phase, the contents of both reactors were mixed, followed by bioaugmentation of one of the two reactors while the other reactor was used as nonaugmented control. *A. communis* $Rif^r$-mSc was pregrown overnight in TSB supplemented with 100 mg $L^{-1}$ rifampicin and 20 mg $L^{-1}$ gentamycin at the operating conditions stated before, washed twice in sterile filtered permeate to remove all antibiotics, and finally resuspended in sterile filtered permeate upon augmentation. Two 200 µL replicates of this cell suspension were dried for 2 h at 105 °C to estimate the amount of augmented biomass. A timescale of the bioaugmentation events is provided in Figure 4.


**Figure 4** | Timescale of bioaugmentation. Day 0 is the first day of augmentation. Two series of augmentation events were performed from day 0 to day 14 and from day 24 to day 31. Reactor analysis was performed before augmentation on the same day.

### 2.5. Survival and persistence of augmented *A. communis* in the MBR

The number of augmented bacteria was monitored by counting their CFU on selective media as a proxy for the number of viable mutants in the reactor. First, sludge samples were deflocculated using a manual tissue grinder (VWR) or ultrasonication. Then, CFU enumeration was performed using TSA plates with antibiotics and 50 µg $mL^{-1}$ of the antifungal additive nystatin. In addition, the location and morphology of the augmented bacteria were visualized by phase contrast and fluorescence microscopy using an Olympus IX83 inverted microscope equipped with a U-FGWA and U-FYW mirror unit. All recipients containing the fluorescent mutant, including the Erlenmeyers and reactor vessel, were shielded from light to avoid bleaching.

### 2.6. Fluorescence *in situ* hybridization

The identity of some bacteria in sludge samples was investigated using FISH as described by Amann (1995) using various oligonucleotide probes targeting *Azoarcus*, *Zoogloea*, and most bacteria (Supplementary material S3). The fluorescence signal was visualized on an Olympus FluoView™ FV1000 confocal microscope.

## 3. RESULTS

### 3.1. Construction and characterization of *A. communis* $Rif^r$-mSc mutant

To enable in-depth monitoring of the augmented strain in the activated sludge with respect to survival and persistence and initial attachment and integration, an antibiotic-resistant and fluorescent mutant strain was constructed.

Rifampicin-resistant mutants developed after 6 days on TSA plates containing 50 mg $L^{-1}$ rifampicin. One mutant was selected as the host strain for fluorescent protein gene insertion. After bi-parental mating of this host and the *E. coli* donor, growth of transconjugants was observed within 4–7 days on LB and TSA plates containing 20 mg $L^{-1}$ gentamycin and 100 mg $L^{-1}$ rifampicin. Roughly 50% of these transconjugants effectively expressed the mScarlet-I fluorescent protein. Alignment revealed that the $Rif^r$-mSc strain showed 99.63% sequence similarity with *A. communis* Swub3. Therefore, this mutant was selected for future experiments.

Within the scope of the reactor experiment, the impact of the introduced mutations on growth rate and amyloid-like substances production was assessed, as a lower growth rate would increase the chance of washout after bioaugmentation. The growth rate of the *A. communis* $Rif^r$-mSc mutant was lower ($0.342 \pm 0.006\ h^{-1}$) compared to that of the wild-type ($0.464 \pm 0.040\ h^{-1}$) (Supplementary material S4). ThT staining after aerobic growth in TSB and synthetic wastewater, and anoxic incubation in synthetic wastewater, revealed characteristic emission peaks at 490 nm suggesting that the mutant was still capable of amyloid-like substances production. Based on these phenotypic properties the constructed mutant was deemed suitable for the bioaugmentation experiment, although the lower growth rate will have to be taken into account when discussing the obtained results. In general, all studied *A. communis* strains produce a prominent slimy or gel-like fraction when harvested during the exponential growth phase (Figure 5).

**Figure 5** | Gel-like extracellular polymeric substances produced by *Azoarcus communis*. Culture grown aerobically in TSB and harvested via centrifugation during exponential growth.

Finally, the stability of the introduced antibiotic and fluorescent markers was examined to assess if the bioaugmented *A. communis* could be correctly monitored during the long-term reactor experiment.

A total of 11 consecutive transfers, approximately corresponding to 131 generations, were grown in a medium not containing antibiotics. The final culture was plated on TSA and various selective media. The number of colony-forming units per liter on TSA supplemented with 50 mg $L^{-1}$ rifampicin ($5.20E+11 \pm 5.77E+10$) or 20 mg $L^{-1}$ gentamycin ($5.83E+11 \pm 5.34E+10$) was equal to the number on TSA ($5.57E+11 \pm 6.05E+10$) ($p = 0.11106708$ and $p = 0.476912649$, respectively, both $> 0.05$). Less growth, but not significantly less, was observed on TSA supplemented with 100 mg $L^{-1}$ rifampicin ($4.87E+11 \pm 4.42E+10$) or 100 mg $L^{-1}$ rifampicin and 20 mg $L^{-1}$ gentamicin ($4.70E+11 \pm 7.00E+10$) ($p = 0.063173788$ and $p = 0.075087307$, respectively, both $> 0.05$). These results suggest that all antibiotic resistance markers were stably inherited by later generations, but too high concentrations of rifampicin inhibited complete recovery. Moreover, slower growth was observed in plates containing 100 mg $L^{-1}$ rifampicin. Additionally, the impact of the antifungal additive nystatin was assessed indicating no effect on recovery. The number of colony-forming units on TSA supplemented with 50 mg $L^{-1}$ nystatin ($5.10E+11 \pm 2.52E+10$) was equal to the number on TSA ($p = 0.155103406 > 0.05$).

The stable inheritance of the mScarlet-I gene after 131 generations was assessed by fluorescence microscopy on 20 colonies, randomly picked from TSA plates, and TSA plates supplemented with 20 mg $L^{-1}$ gentamicin or 100 mg $L^{-1}$ rifampicin and 20 mg $L^{-1}$ gentamicin. All colonies appeared fluorescent using the U-FGWA and U-FYW filter set indicating the persistent presence of the mScarlet-I fluorescent protein gene.

### 3.2. Flocculation properties

The bioflocculant capacity of *A. communis* $Rif^r$-mSc and *E. coli* mutants was estimated against two model systems. The flocculation activity index (FAI, Figure 6) is calculated from the absorbance of the supernatants

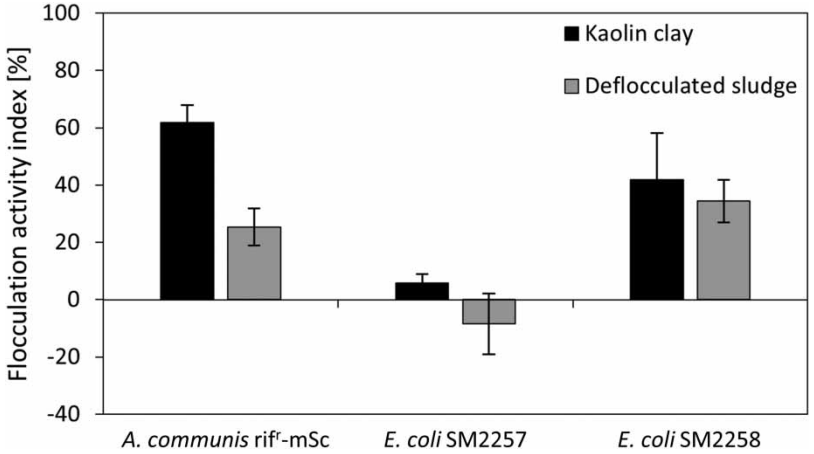


**Figure 6** | Flocculation activity against kaolin clay suspension and deflocculated activated sludge. After inoculation at an initial $OD_{600}$ of 0.05, *Azoarcus communis* Rif$^r$-mSc was grown in tryptic soy broth for 16.5 h, and the *Escherichia coli* SM2257 curli-deficient mutant and SM2258 mutant with upregulated curli production were grown in M63 broth for 48 h. Each value represents the average of three biological replicates. Error bars represent standard deviations.

which is the result of multiple interactions. These interactions can positively (e.g., bridging) or negatively (e.g., hindered settling) affect the FAI. Against a kaolin clay suspension, the highest flocculating activity was observed for *Azoarcus* (61.8%), followed by *E. coli* SM2258 mutant with upregulated curli production (41.8%) and *E. coli* SM2257 curli-deficient mutant (5.91%). Similar trends were observed against a deflocculated sludge suspension. Negative values for curli-deficient *E. coli* indicate a hindered settling, counteracting any present flocculation effect. These experiments were conducted in PBS with a pH of 7.4, which is similar to the average pH in the MBR reactors.

### 3.3. MBR: startup phase

Prior to augmentation, the parallel MBRs were operated for 40 days to allow the microbial community to adapt to the changed environment. Floc morphology and ThT emission were quantified at regular timepoints to (*i*) confirm stationarity of these parameters before augmentation and (*ii*) confirm equal reactor conditions. The ThT emission signal quickly increased in both MBRs compared to the inoculum until an equilibrium was achieved at the end of the startup phase (Figure 7). The average floc size increased (Figure 8) compared to the inoculum. These quantified parameters roughly stabilized after 40 days, which equals twice the sludge retention time (SRT)

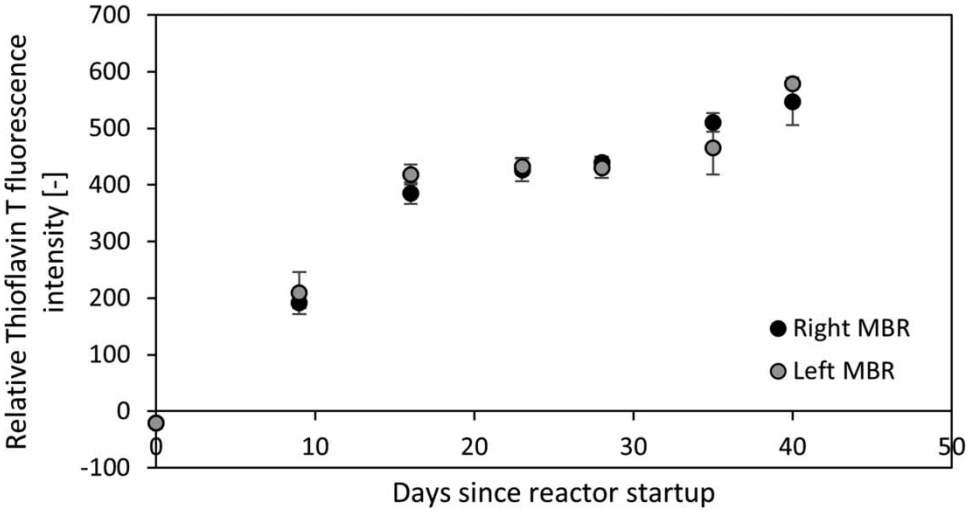


**Figure 7** | Evolution of ThT fluorescence intensity at 490 nm in the MBRs. Sample stained with 3-μM ThT relative to unstained sample. Each value represents the average of four technical replicates.

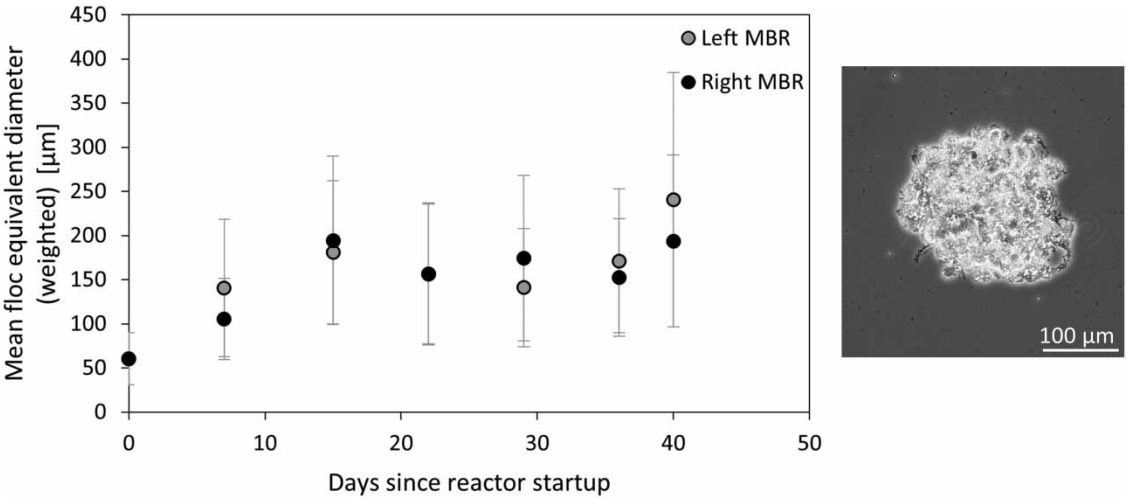


**Figure 8** | Sludge morphology. Evolution of the average equivalent floc diameter in the MBRs (left). Error bars represent standard deviations. Activated sludge floc with representative morphology taken from the left MBR at day 40 in phase contrast (right).

of 20 days. Similar trends were observed for all quantified parameters for both reactors, indicating similar conditions. Therefore, it is assumed that changes observed later can be attributed to the effect of bioaugmentation.

### 3.4. MBR bioaugmentation: survival and persistence and behavior of the *A. communis* mutant

At the end of the 40-day startup period, communities were mixed once to ensure equal conditions for both bioreactors. One MBR was augmented with *A. communis* Rif$^r$-mSc and another served as a nonaugmented reference reactor. Two series of augmentation events took place: by day 14, a total of 1.20 g *A. communis* had been added to the reactor followed by an additional 2.15 g by day 31. To compare, the average total sludge content in the augmented reactor during the augmentation phase was 13.38 g. Note that all following results have been represented at 'days since the start of augmentation'.

The survival and persistence of *A. communis* Rif$^r$-mSc after bioaugmentation was monitored using two methods. Firstly, deflocculated mixed liquor samples were plated on TSA with 20 mg $L^{-1}$ gentamycin, 100 mg $L^{-1}$ rifampicin, and 50 mg $L^{-1}$ nystatin. No growth was observed for samples from the reference reactor, indicating that no indigenous organisms could grow on these selective plates. This observation, together with the observed stable inheritance of the introduced mutations (see Section 3.1), suggests that the enumeration of the colony-forming units was a good estimate for the number of viable *A. communis* Rif$^r$-mSc in the augmented reactor (Figure 9). Note that at first, CFU was quantified only once before the next

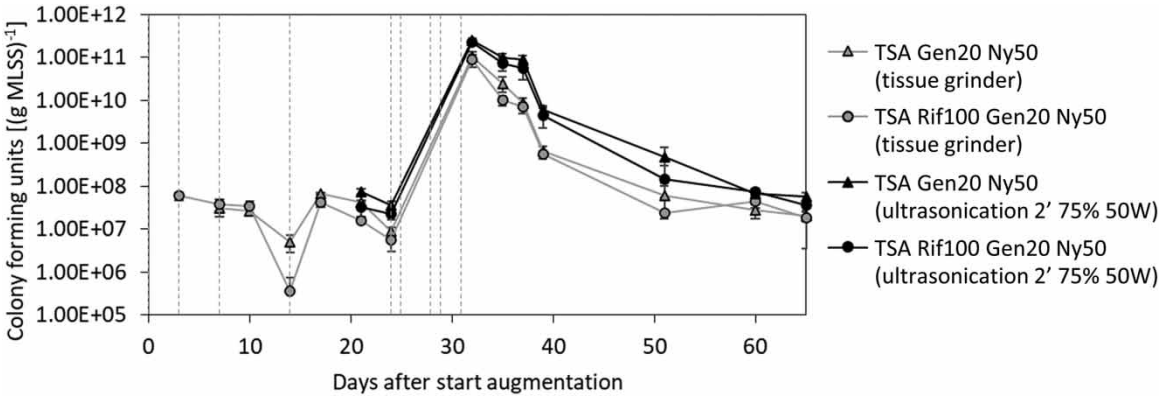


**Figure 9** | Evolution of colony-forming units in the augmented MBR. Deflocculated samples were grown on tryptic soy agar plates containing 20 mg $L^{-1}$ gentamycin, 100 mg $L^{-1}$ rifampicin, and 50 mg $L^{-1}$ nystatin selective for *Azoarcus communis* Rif$^r$-mSc. Dashed lines indicate the bioaugmentation events. Analyses were performed prior to augmentation on the same day. Each value represents the average of six technical replicates.

bioaugmentation event, giving no information about the *A. communis*' faith after bioaugmentation. Only data from days 10 and 14, days 17–24, and starting from day 32 can be used for this purpose. Moreover, deflocculation using a manual tissue grinder resulted in a less complete deflocculation and subsequent underestimation for the CFU compared to deflocculation with ultrasound that was introduced on day 21. Similarly, growth on plates containing 100 mg $L^{-1}$ rifampicin mostly resulted in a lower number of CFU compared to the plates without rifampicin that were introduced on day 7. By any means, the concentration of *A. communis* decreased after bioaugmentation but finally stagnated at ca. $1 \times 10^8$ CFU (g MLSS)$^{-1}$ around 25 days after the last bioaugmentation event in all datasets.

Secondly, sludge samples were studied using fluorescence microscopy. The exposure time and light sensitivity were chosen such that all observable autofluorescence in a sample from the reference reactor was minimized using the U-FGWA filterset. In this way, the fluorescent mScarlet-I protein expressed by the augmented strain could be visualized. This observation method was combined with phase contrast microscopy to roughly monitor its abundance, and also gain information about its spatial distribution within the sludge floc (Figure 10). After the first bioaugmentation stage, almost no fluorescent spots were observed (such as in Figure 10, day 17). After the second bioaugmentation stage, *Azoarcus* was observed as single bacteria or larger fluorescent clusters. The single bacteria were all seemingly adsorbed onto the floc surface (such as in Figure 10, day 32 image A). Later, larger fluorescent spots were observed onto and within sludge flocs (such as in Figure 10, day 44). These spots most probably corresponded to microcolonies of *A. communis* Rif$^r$-mSc grown from the initially attached single bacteria. Later, little fluorescence was observed (such as in Figure 10, day 65). Large clusters were observed either loose or integrated into the floc (such as in Figure 10, day 32 image B) and thought to be due to incomplete resuspension after washing before augmentation. Within 1 day after bioaugmentation, fluorescence was detected within several rotifers (such as in Figure 10, day 8 images A and B and day 32, detail framed in blue) and to a lesser extent in stalked ciliates (such as in Figure 10, day 32, detail framed in red).

### 3.5. MBR bioreactor bioaugmentation: impact on amyloid-like content and bioflocculation performance

ThT staining was performed to investigate the amyloid-like material in the sludge flocs augmented with *A. communis* Rif$^r$-mSc (Figure 11). The U-FYW filterset was used to detect the mScarlet-I while avoiding crosstalk from the lower wavelength emission signal from the ThT. The exposure time and light sensitivity were chosen such that all observable autofluorescence in a sample from the reference reactor was minimized in the BFP and U-FYW filtersets. At 1 and 8 days after the last bioaugmentation (day 32 and day 39, respectively), the ThT emission signal was lower where *A. communis* Rif$^r$-mSc was located compared to the rest of the floc. Later (e.g., at day 44), the fluorescent mutant was only found completely embedded in the floc such that its ThT fluorescence could not be assessed using the IX83 microscope. Quantification of the ThT emission signal revealed a rather fluctuating signal (Figure 12). No effect that might be attributed to the augmentation of *A. communis* was observed, which is not unexpected given its low abundance in the augmented reactor.

Image analysis was performed to assess the impact of augmentation on the bioflocculation performance. The number-based particle size distribution (Figure 13, left) shows that the frequency of the smallest particle class representing single bacteria did not increase in the augmented MBR on day 32, a day after the second series of augmentation events. These particle size distributions suggest that within 24 h, most *Azoarcus* supplemented in suspension were either attached to other biomass within 24 h or consumed by other organisms. The surface-based particle size distribution (Figure 13, right) shows that the frequency of the larger particle classes increases at days 32 and 39 compared to the reference MBR but the overall results indicate a rather large variability for both reactors. Therefore, no trends could be attributed to the augmentation of *Azoarcus*.

The bacterial community composition was investigated via FISH (Figure 14) to identify indigenous organisms that might fulfill the same metabolic function (denitrifiers) or structural function (structural EPS producers). The mScarlet-I protein expressed by the augmented *A. communis* Rif$^r$-mSc mutant was still detectable after the FISH procedure. Simultaneous binding with AZA645 and AT1458 indicates *Azoarcus*. These results suggested that no indigenous *Azoarcus* were present in the reactor: all areas targeted simultaneously by both probes also showed mScarlet-I fluorescence. Binding with AZA645-only indicates the presence of some *Rhodocyclus* or *Dechloromonas*. Binding with AT1458-only indicates the presence of *Thauera*. Also *Zoogloea* was detected in the MBR sludge with the ZRA23a oligonucleotide probe.

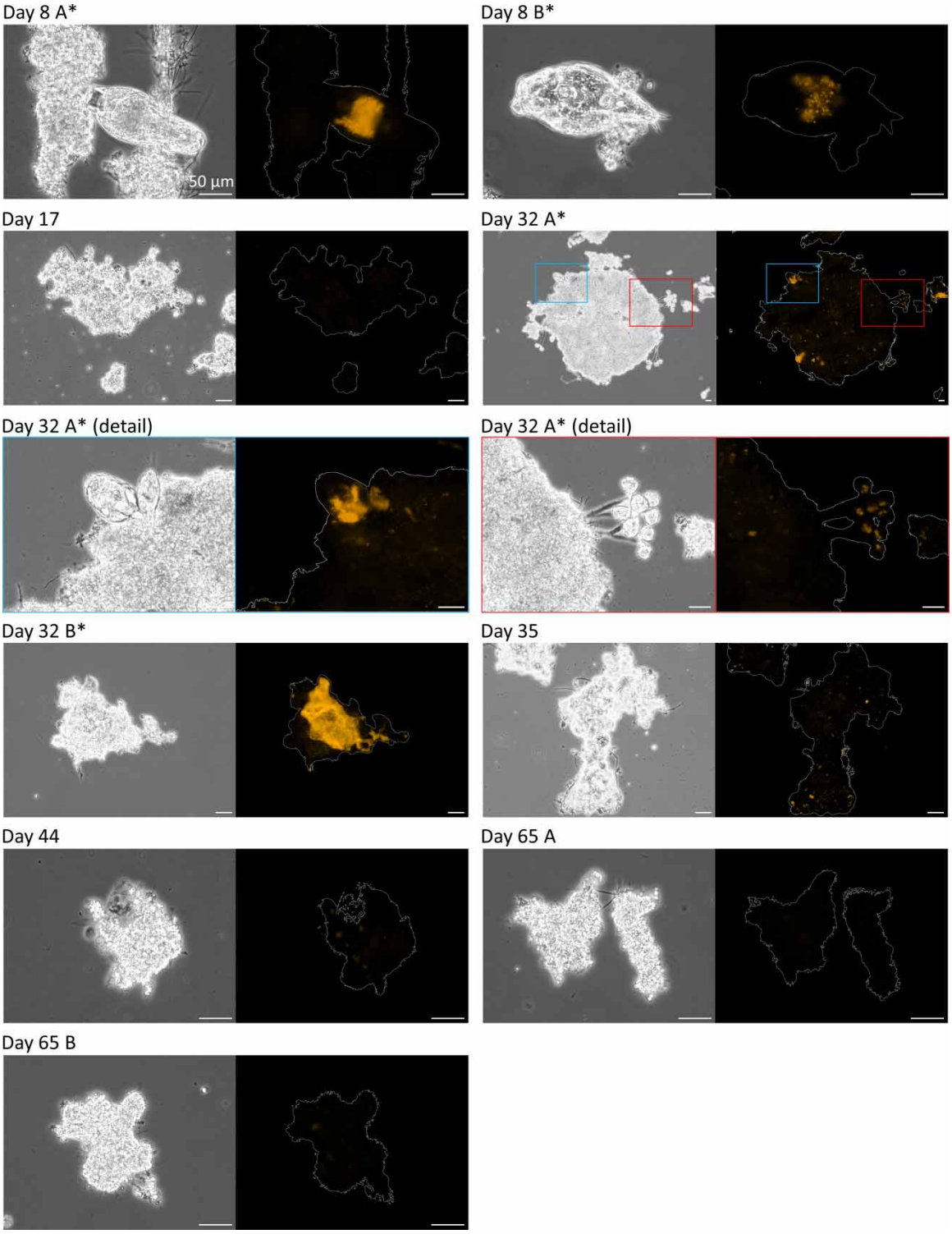


**Figure 10** | Epifluorescence and phase contrast images illustrating the abundance and location of *Azoarcus communis* Rif$^r$-mSc in sludge flocs in the MBR. Images shown during augmentation (days 8 and 17 after the start of augmentation) and later. Images are representative unless when indicated with an asterisk (*). Analyses were performed prior to augmentation on the same day. To improve visibility, the outline of the floc is superimposed on the fluorescence image. All scale bars = 50 µm. Please refer to the online version of this paper to see this figure in colour: https://dx.doi.org/10.2166/wpt.2023.103.

## 4. DISCUSSION

This experiment aims to assess the impact of structural EPS on activated sludge flocculation by actively adding a structural EPS producer. Traditionally, inorganic and synthetic flocculants are used for bioflocculation

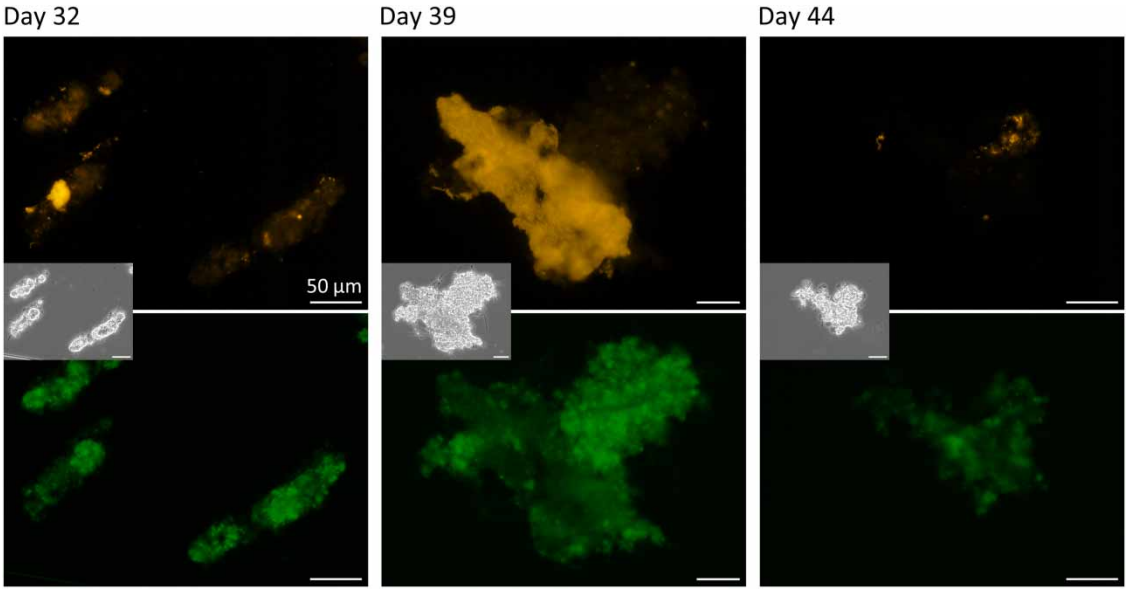


**Figure 11** | Fluorescence and phase contrast images of sludge flocs stained with 10 µM ThT. Samples taken from the MBR augmented with *Azoarcus communis* Rif$^r$-mSc (mScarlet-I protein, orange) and stained with 10 µM ThT (green). Results shown after the last augmentation (days counted since the start of augmentation). Flocs were selected for their high abundance of mScarlet-I and are thus not representative. All scale bars = 50 µm. Please refer to the online version of this paper to see this figure in colour: https://dx.doi.org/10.2166/wpt.2023.103.

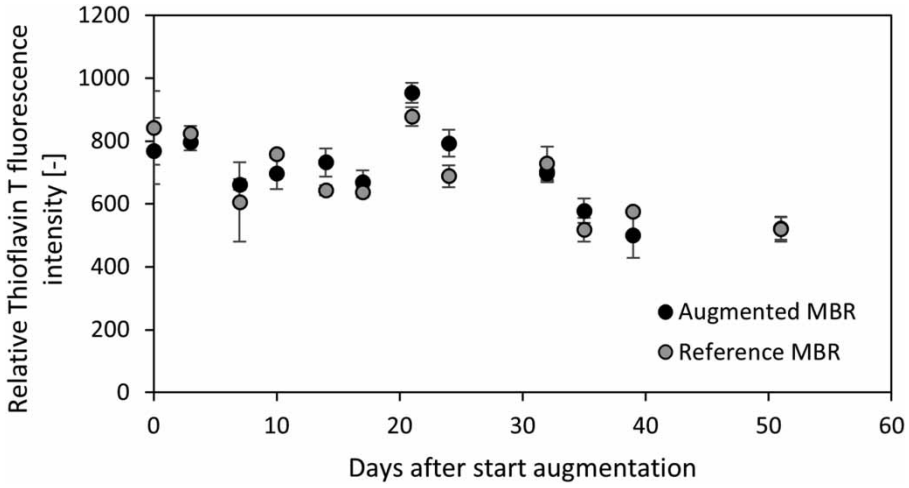


**Figure 12** | Evolution of ThT fluorescence intensity at 490 nm in the bioaugmented and reference MBR. Sample stained with 10 µM ThT relative to unstained sample. Each value represents the average of four technical replicates.

remediation. However, these flocculants are associated with a lack of biodegradability and with health hazards (Lee *et al.* 2014). Bioflocculants, i.e., natural polymers extracted from bacteria or other sources, are being investigated as an alternative but their commercialization is hampered due to their higher production cost (Liu *et al.* 2010). Moreover, (bio)flocculants add to the waste sludge volume and have to be reapplied regularly. If the abundance of flocculants in the activated sludge system can be increased by adding (or stimulating) a bioflocculant producer, these disadvantages are avoided. In fact, the bioflocculant producer can play an active role in the biodegradation of pollutants and maintain its presence in the sludge through growth.

A case study is presented involving *A. communis*, a denitrifier with amyloid-like substances production and flocculation potential. In view of monitoring the augmented strain, the introduction of biological markers and their stability are discussed. Since these markers indicated that only a low fraction of augmented bacteria was sustained in the system after augmentation, adaptations to the approach are suggested.

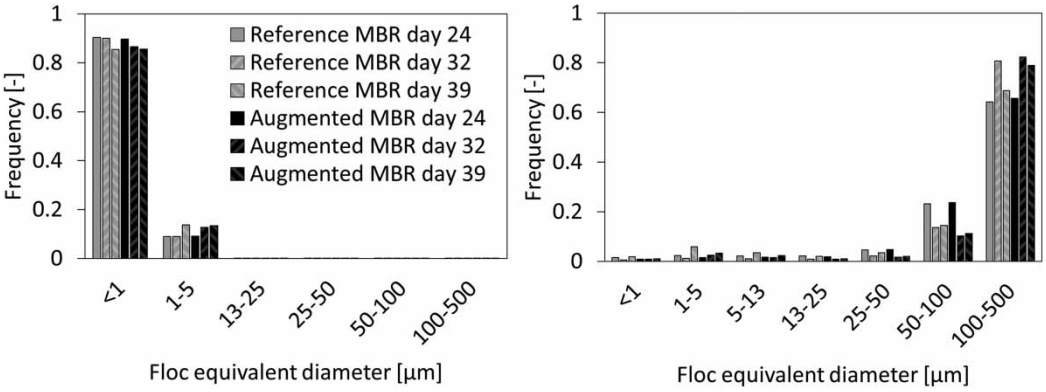


**Figure 13** | Evolution of the number-based (left) and surface-based (right) sludge particle size distribution in the bioaugmented and reference MBRs.

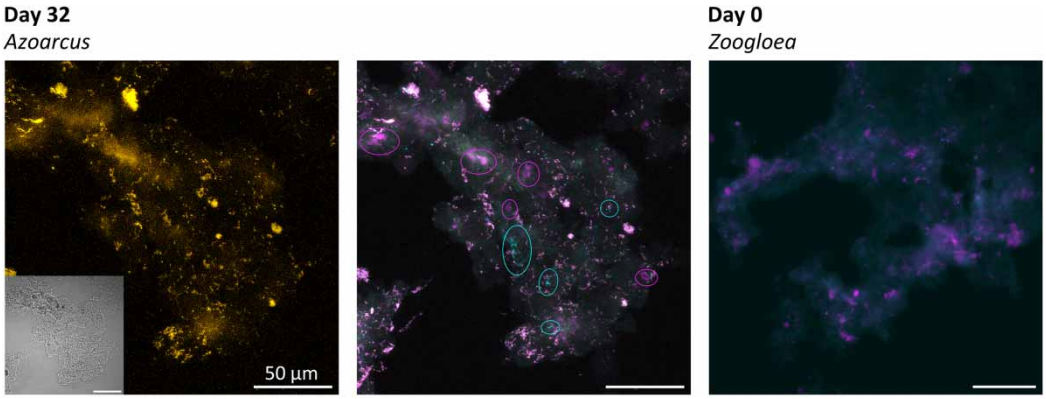


**Figure 14** | Representative fluorescence images illustrating the spatial distribution of indigenous organisms and augmented *Azoarcus communis* in sludge flocs in the augmented MBR. Day 32: left: *Azoarcus communis* Rif$^r$-mSc represented in orange. Right: sample stained with oligonucleotide probes targeting most *Azoarcus* and some uncultured *Rhodocyclus* and *Dechloromonas* (AZA645, magenta) and the *Azoarcus-Thauera* cluster (AT1458, cyan). AZA645-only and AT1458-only areas indicated in magenta or cyan. Day 0: left: sample stained with probes targeting most *Zoogloea* (ZRA23a, magenta) and *Bacteria* (EUBmix, cyan). Days counted since the start of augmentation. All *Azoarcus* images are CLSM z-stacks represented as maximum intensity projections. Please refer to the online version of this paper to see this figure in colour: https://dx.doi.org/10.2166/wpt.2023.103.

### 4.1. Structural EPS production and flocculation activity

ThT staining suggested that *A. communis* was capable of producing amyloids when grown in monoculture in TSB or in synthetic wastewater. To our knowledge, this research provides the first evidence of Thioflavinophilic EPS production of a monoculture of a specific species of the genus *Azoarcus*. Additional research using other analytical methods (e.g., FT-IR) should be considered to (*i*) check the specificity of the ThT dye, which is prone to unspecific binding to, e.g., cellulose fibers (Retna Raj & Ramaraj 2001), and (*ii*) identify EPS-components besides amyloids. Such components are expected to be present based on visual observation of a prominent slimy or gel-like fraction when *A. communis* is harvested during the exponential growth phase.

The short-term impact on flocculation was assessed against two types of samples and using either *A. communis* or one of two reference strains: *E. coli* with upregulated curli production and a curli-deficient *E. coli* mutant. These three strains are referred to as 'bioflocculant producers' in this paragraph. In these experiments, the bioflocculants are added together with their producing strain, without prior extraction and purification steps. Removal of growth medium, washing, and resuspension in PBS are the only pretreatment steps. This approach differs from much other work regarding bioflocculants but omits extra preparation time. The turbidity of the clarifying suspension of kaolin and bioflocculant producer was more strongly decreased in case of *A. communis* and *E. coli* with upregulated curli production compared to the *E. coli* curli-deficient mutant. This can be the result of several flocculating mechanisms dependent on the nature of the bioflocculant such as (*i*) bridging mediated by

cations and charge neutralization in case of cation-dependent bioflocculants or (*ii*) direct attachment and bridging in case of cation-independent bioflocculants (Lian *et al.* 2008; Li *et al.* 2009; Liu *et al.* 2010). Lower flocculation activity was observed against deflocculated sludge but the trends remained similar. It should be noted that the interpretation of these results is more complex due to (*i*) potential sludge reflocculation, (*ii*) potential incomplete deflocculation providing less sludge surface area to bind to, and (iii) general heterogeneity of the sludge sample. Moreover, the ultrasonication of the sludge might result in partial extraction of its EPS. Therefore, the FAI measures the combined flocculation effect of sludge on *A. communis* and of *A. communis* on sludge. Overall, these experiments suggest that amyloids benefit the flocculation activity of a strain, making *A. communis* an interesting candidate for the augmentation experiment. As another potential application, *A. communis* might be utilized for short-term activated sludge recovery during a deflocculation event, yet this application was not investigated. Repetitions using different sludge samples and different amyloid-producing and -deficient strains should be considered for further research to evaluate the generalizability of these results.

Based on these results, it is recommended to consider the structural EPS-producing capacity and, more specifically, amyloid-producing capacity to evaluate candidate strains for bioaugmentation aiming to improve bioflocculation, among other factors. The proposed ThT staining procedure might be used in this context. This recommendation corresponds to the use of Congo Red as a reagent to select microorganisms for flocculant production as an alternative to synthetic polymers (Rebah *et al.* 2018).

### 4.2. Evolution of ThT fluorescence intensity and floc size in the MBR

The startup phase of MBR operation coincided with a quick increase of ThT fluorescence in the sludge compared to the inoculum. This observation suggests that the amyloid-like content has increased. The startup phase also coincides with an increased floc size. Thus, after 40 days of MBR operation, *A. communis* was introduced into well-flocculating and amyloid-like substances-rich sludge as a baseline.

### 4.3. *A. communis* bioaugmentation and impact on ThT fluorescence intensity and floc size

Two series of augmentation events were performed and the presence of the augmented strain was monitored qualitatively via fluorescence microscopy and quantitatively via the enumeration of colony-forming units. After the second augmentation series, fluorescent clusters were observed, seemingly grown from single adsorbed cells, and at the end of reactor operation, the number of colony-forming units stabilized.

These two observations suggest that some of the augmented *A. communis* stably established themselves in the sludge and were actively growing. However, only a minor fraction of the augmented bacteria survived. Three potential explanations are presented here. Firstly, the presence of indigenous microorganisms that fill the same metabolic ecological niche might have led to competition for *A. communis*. 16S rRNA gene sequencing indeed revealed the presence of several denitrifiers, including *Azoarcus*, in a sample from the same origin as the reactor inoculum, and *Zoogloea* has been detected in the MBR using FISH. Moreover, Wilderer *et al.* (1991) have suggested that it may be more difficult for an inoculated bacterial strain to outcompete the indigenous bacteria if the latter are fully adapted to the environment. Furthermore, the mScarlet-I mutant has a significantly lower growth rate compared to the wild-type *Azoarcus*. It should be noted that *A. communis*, like other plant-associated *Azoarcus* species, grows well on salts of organic acids and aromatic substrates but cannot metabolize carbohydrates (Reinhold-Hurek *et al.* 1993). Glucose thus remains available in the synthetic wastewater to be consumed by, e.g., other denitrifiers. Secondly, since bacteria were augmented in suspension, and were observed to be adsorbed onto the outside of the flocs after 24 h, metazoan and protozoan grazing might have contributed to the decline of the augmented *Azoarcus*. In this case, mScarlet-I fluorescence was detected within several rotifers and to a lesser extent in stalked ciliates that are both able to consume whole bacteria (Cybis & Horan 1997). The effect of grazing should not be underestimated: the work by Bouchez *et al.* (2000) points toward grazing by ciliates and other protozoa as the main reason for the failure of bioaugmentation of an aerobic denitrifying bacterium augmented in a nitrifying acetate-fed SBR. Thirdly, several abiotic factors might have adversely impacted the survival of the augmented *A. communis*. While growth on synthetic wastewater in aerobic conditions was confirmed in preliminary experiments, these batch experiments did not account for the cyclic nutrient and pH variations in the reactor, the hydrodynamics caused by bubble aeration, or the operating temperature of around 24 °C instead of 28 °C.

ThT fluorescence intensity was relatively low in the regions where *A. communis* was embedded suggesting a lower amyloid-like content in these regions. With this assumption in mind, two possible explanations are

proposed. Firstly, several abiotic factors might have hampered the amyloid-like substances production of *A. communis* in the reactor. As elaborated before, the preliminary experiments showing that amyloid-like substance production occurred in synthetic wastewater in aerobic and anoxic conditions did not perfectly mimic the reactor conditions. Secondly, the identified *A. communis* might be predominantly dead and thus unable to produce amyloid-like EPS. This hypothesis can be tested using cell-impermeable nucleic acid stains indicating compromised membranes. However, the in-house available SYTOX Orange and Propidium Iodide stains were not suitable for this purpose because of partial spectral overlap with mScarlet-I.

However, augmentation of this strain did not lead to measurable effects on the reactor sludge morphology after 24 h and longer. This discrepancy might be caused by the already excellent flocculation status of the reactor sludge at the time of augmentation providing few single cells or light small flocs to bind to. Again, a higher fraction of augmented bacteria in the sludge might have led to clearer effects. In total 3.33 g of *A. communis* was added gradually to 13.38 g of reactor biomass while Xin *et al.* (2017) added as much as 13 g of TN-14 to 3.3 g of conventional sludge to facilitate aerobic granulation.

### 4.4. Comments on the applied procedures

*Antibiotic resistance.* Antibiotic resistance is an effective tool for monitoring the survival and persistence of an augmented strain in activated sludge but is clearly a monitoring tool limited to the laboratory. Given that the presence of antibiotic-resistant organisms in the environment can contribute to a public health problem (e.g., Zaman *et al.* 2017), it is not appropriate to use such an approach to monitor augmentation in full-scale systems. In these full-scale systems, the augmentation should be performed with the wild-type strain. Evidently, in laboratory-scale experiments, it is necessary to handle antibiotic-containing growth media and antibiotic-resistant organisms properly, i.e., by autoclaving prior to disposal.

*Flocculation activity index.* Results for the flocculation activity index (FAI) against kaolin cannot be compared to the literature because of the adapted equation for FAI accounting for the contribution of the bioflocculant producer to the absorbance. Moreover, the absorbance was measured after 5 min of settling instead of 1. With this method, the bioflocculant producers investigated in this study might often appear more effective, while in reality a prolonged settling time was required to even obtain a measurable effect. Finally, the pipetting of the supernatant appeared very prone to human error as shown in the large standard deviation for three separate measurements for $A_{550}$ of the same deflocculated activated sludge sample ($0.660 \pm 0.092$, $N = 3$).

### 4.5. Future work

Only a small fraction of the augmented bacteria survived in the bioreactor such that their hypothesized impact on amyloid-like content and bioflocculation could not be assessed. Competition, grazing, and abiotic factors might have hampered the survival and persistence of *A. communis*. Three modifications to the experimental design and bioaugmentation approach are formulated here to assess these concerns. Firstly, future bioreactor experiments might operate the reactor without a membrane but with a short settling phase followed by effluent removal from the top. This method of hydraulic selective pressure and washout is often used to promote granulation from floccular sludge (Qin *et al.* 2004a, 2004b). This adaptation to the reactor mechanical design and operation will thus select for the best settling flocs and is hypothesized to give a selective advantage to the EPS-producing augmented strain. Indeed, the potential presence of indigenous denitrifiers did not provide *A. communis* with enough sufficient selective advantage to establish itself in the reactor based on its denitrifying function. Still, we suggest using a membrane during the first 24 h after augmentation to give suspended cells the time to adhere and avoid their washout. Secondly, while the membrane cell retention system avoided the washout of suspended cells including *A. communis*, it did not protect the bacteria from metazoan and protozoan grazing. Future work might therefore use the embedding of bacteria within an alginate matrix as another cell retention strategy. This embedding has proven to be successful against protozoan grazing in a nitrifying laboratory-scale reactor augmented with an aerobic denitrifying bacterium (Bouchez *et al.* 2009). Thirdly, while *A. communis* could not thrive under the abiotic conditions present in the reactor, other EPS-producing denitrifiers might. Future research might rely on 16S rRNA sequencing of samples stored from this experiment to select dominant potential amyloid-producing genera for augmentation.

In terms of cost and efficiency, this direct augmentation of EPS producers (presumably with alginate) will be more suitable for other higher added-value biotechnology applications, where competition is lower and influent conditions are more controlled. Potential applications include sand filters for drinking water production (aimed

at removing specific micropollutants or other emerging contaminants), the retention of non-flocculating bacteria (that will then form an aggregate through the bioflocculant producing microorganism), and the harvesting of microalgae (Jiang *et al.* 2006; Lee *et al.* 2009; Wang *et al.* 2021). For full-scale activated sludge systems, the promotion of native structural EPS producers and their structural EPS production by adjusting the operating conditions is still preferred over bioaugmentation.

## 5. CONCLUSION

This study aimed to explore the impact of structural EPS on bioflocculation of activated sludge by augmentation of a structural EPS producer. The selected *A. communis* strain was shown to produce gel-like material with thioflavinophilic properties, suggesting the presence of amyloid adhesins. *A. communis* was thus identified as a proper candidate for the proposed augmentation experiment, thereby confirming the first research hypothesis. Augmentation of *Azoarcus* was performed gradually over 31 days. Enumeration of colony-forming units on selective agar plates supplemented with antibiotics suggested that only a fraction of augmented *Azoarcus* survived. Three explanations were proposed: competition with indigenous organisms filling the same metabolic function (denitrifiers), grazing by rotifers and ciliates, and unfavorable abiotic conditions were proposed as explanations. Grazing was visually confirmed through the detection of the *Azoarcus*-produced mScarlet-I fluorescent protein emission inside these organisms. As a result of the low abundance of augmented *Azoarcus* in the bioreactor, the hypothesized beneficial impact on amyloid-like content (hypothesis 2) and bioflocculation performance (hypothesis 3) could not be assessed.

A framework with two recommendations for future bioaugmentation experiments aiming to improve bioflocculation was established. Firstly, the construction of a fluorescent protein-producing mutant is recommended. This modification enables microscopic monitoring of the location of the augmented bacteria in the sludge floc, which might bring valuable insights into the initial attachment and further integration processes. The stable inheritance of this fluorescent marker was confirmed in the studied Gram-negative strain. Secondly, structural EPS-producing capacities should be included as a criterium for strain selection. Short-term experiments demonstrate the beneficial impact of *Azoarcus* and amyloid-producing *E. coli* strains on the flocculation of clay and deflocculated sludge.

## ACKNOWLEDGEMENTS

An-Sofie Christiaens holds a PhD grant for Strategic Basic Research from the Research Foundation-Flanders (FWO-1S41422N). Aquafin (Belgium) is acknowledged for providing sludge. We thank Daniel Otzen (Aarhus University) for the *E. coli* K-12 mutants, Ivo Vankelekom and Ayesha Ilyas (KU Leuven) for the fabrication of the membranes, Dirk Springael, Tran Quoc Tran, and Tinh Nguyen Van (KU Leuven) for enabling the transposon mutagenesis and help with Sanger sequencing, Tom Van Gerven (KU Leuven) for providing access to the ultrasonic processor, Johan Martens (KU Leuven) for providing access to the microplate reader, and Johan Hofkens and Rik Nuyts (KU Leuven) for providing access to the confocal microscope.

## DATA AVAILABILITY STATEMENT

All relevant data are available from an online repository. The repository can be accessed via: https://doi.org/10.48804/ROBCTI.

## CONFLICT OF INTEREST

The authors declare there is no conflict.

## REFERENCES

Altschul, S. F., Gish, W., Miller, W., Myers, E. W. & Lipman, D. J. 1990 Basic local alignment search tool. *Journal of Molecular Biology* **215**(3), 403–410. https://doi.org/10.1016/S0022-2836(05)80360-2.

Amann, R. 1995 In situ identification of micro-organisms by whole cell hybridization with rRNA-targeted nucleic acid probes. In: *Molecular Microbial Ecology Manual*. https://doi.org/10.1007/978-94-011-0351-0_23.

An, W., Guo, F., Song, Y., Gao, N., Bai, S., Dai, J., Wei, H., Zhang, L., Yu, D., Xia, M., Yu, Y., Qi, M., Tian, C., Chen, H., Wu, Z., Zhang, T. & Qiu, D. 2016 Comparative genomics analyses on EPS biosynthesis genes required for floc formation of *Zoogloea resiniphila* and other activated sludge bacteria. *Water Research* **102**, 494–504. https://doi.org/10.1016/j.watres.2016.06.058.

Bouchez, T., Patureau, D., Dabert, P., Juretschko, S., Doré, J., Delgenès, P., Moletta, R. & Wagner, M. 2000 Ecological study of a bioaugmentation failure. *Environmental Microbiology* **2**(2), 179–190. https://doi.org/10.1046/j.1462-2920.2000.00091.x.

Bouchez, T., Patureau, D., Delgenès, J. P. & Moletta, R. 2009 Successful bacterial incorporation into activated sludge flocs using alginate. *Bioresource Technology*. https://doi.org/10.1016/j.biortech.2008.07.028.

Christiaens, A., van Steenkiste, M., Rummens, K. & Smets, I. 2022 Amyloid adhesin production in activated sludge is enhanced in lab-scale sequencing batch reactors: feeding regime impacts microbial community and amyloid distribution. *Water Research X* **17**, 100162. https://doi.org/10.1016/j.wroa.2022.100162.

Cybis, F. D. A. & Horan, N. J. 1997 Protozoan and metazoan populations in sequencing batch reactors operated for nitrification and/or denitrification. *Water Science and Technology* **35**(1), 81–86. https://doi.org/10.1016/S0273-1223(96)00882-7.

de Lorenzo, V., Herrero, M., Jakubzik, U. & Timmis, K. N. 1990 Mini-Tn5 transposon derivatives for insertion mutagenesis, promoter probing, and chromosomal insertion of cloned DNA in gram-negative eubacteria. *Journal of Bacteriology* **172**(11), 6568–6572. https://doi.org/10.1128/jb.172.11.6568-6572.1990.

Demir, I., Besson, A., Guiraud, P. & Formosa-Dague, C. 2020 Towards a better understanding of microalgae natural flocculation mechanisms to enhance flotation harvesting efficiency. *Water Science and Technology* **82**(6), 1009–1024. https://doi.org/10.2166/wst.2020.177.

Dueholm, M. K. D., Nierychlo, M., Andersen, K. S., Rudkjøbing, V., Knutsson, S., Arriaga, S., Bakke, R., Boon, N., Bux, F., Christensson, M., Chua, A. S. M., Curtis, T. P., Cytryn, E., Erijman, L., Etchebehere, C., Fatta-Kassinos, D., Frigon, D., Garcia-Chaves, M. C., Gu, A. Z., Horn, H., Jenkins, D., Kreuzinger, N., Kumari, S., Lanham, A., Law, Y., Leiknes, T. O., Morgenroth, E., Muszyński, A., Petrovski, S., Pijuan, M., Pillai, S. B., Reis, M. A. M., Rong, Q., Rossetti, S., Seviour, R., Tooker, N., Vainio, P., van Loosdrecht, M., Vikraman, R., Wanner, J., Weissbrodt, D., Wen, X., Zhang, T., Albertsen, M. & Nielsen, P. H. 2022 MiDAS 4: a global catalogue of full-length 16S rRNA gene sequences and taxonomy for studies of bacterial communities in wastewater treatment plants. *Nature Communications* **13**(1), 1–15. https://doi.org/10.1038/s41467-022-29438-7.

Dwari, R. K. & Mishra, B. K. 2019 Evaluation of flocculation characteristics of kaolinite dispersion system using guar gum: a green flocculant. *International Journal of Mining Science and Technology* **29**, 745–755. https://doi.org/10.1016/j.ijmst.2019.06.001.

Florey, K. 1976 *Analytical Profiles of Drug Substances*. Academic Press, New York.

Frank, J. A., Reich, C. I., Sharma, S., Weisbaum, J. S., Wilson, B. A. & Olsen, G. J. 2008 Critical evaluation of two primers commonly used for amplification of bacterial 16S rRNA genes. *Applied and Environmental Microbiology* **74**, 2461–2470. https://doi.org/10.1128/AEM.02272-07.

Horecka, J. & Chu, A. M. 2017 *Yeast Colony PCR: It Doesn't Get Any Easier Than This!* pp. 1–4. https://dx.doi.org/10.17504/protocols.io.gzwbx7e.

Jenné, R., Banadda, E. N., Smets, I., Deurinck, J. & Van Impe, J. 2007 Detection of filamentous bulking problems: developing an image analysis system for sludge composition monitoring. *Microscopy and Microanalysis* **13**, 36–41. https://doi.org/10.1017/S1431927607070092.

Jiang, H. L., Tay, J. H., Maszenan, A. M. & Tay, S. T. L. 2006 Enhanced phenol biodegradation and aerobic granulation by two coaggregating bacterial strains. *Environmental Science and Technology* **40**, 6137–6142. https://doi.org/10.1021/es0609295.

Juretschko, S., Loy, A., Lehner, A. & Wagner, M. 2002 The microbial community composition of a nitrifying-denitrifying activated sludge from an industrial sewage treatment plant analyzed by the full-cycle rRNA approach. *Systematic and Applied Microbiology* **25**(1), 84–99. https://doi.org/10.1078/0723-2020-00093.

Kent, T. R., Bott, C. B. & Wang, Z. W. 2018 State of the art of aerobic granulation in continuous flow bioreactors. *Biotechnology Advances* **36**(4), 1139–1166. https://doi.org/10.1016/j.biotechadv.2018.03.015.

Klausen, M. M., Thomsen, T. R., Nielsen, J. L., Mikkelsen, L. H. & Nielsen, P. H. 2004 Variations in microcolony strength of probe-defined bacteria in activated sludge flocs. *FEMS Microbiology Ecology* **50**(2), 123–132. https://doi.org/10.1016/j.femsec.2004.06.005.

Kurane, R., Takeda, K. & Suzuki, T. 1986 Screening for and characteristics of microbial flocculants. *Agricultural and Biological Chemistry* **50**(9), 2301–2307. https://doi.org/10.1080/00021369.1986.10867746.

Larsen, P., Nielsen, J. L., Dueholm, M. S., Wetzel, R., Otzen, D. & Nielsen, P. H. 2007 Amyloid adhesins are abundant in natural biofilms. *Environmental Microbiology*. https://doi.org/10.1111/j.1462-2920.2007.01418.x.

Larsen, P., Nielsen, J. L., Otzen, D. & Nielsen, P. H. 2008 Amyloid-like adhesins produced by floc-forming and filamentous bacteria in activated sludge. *Applied and Environmental Microbiology*. https://doi.org/10.1128/AEM.02274-07.

Lee, A. K., Lewis, D. M. & Ashman, P. J. 2009 Microbial flocculation, a potentially low-cost harvesting technique for marine microalgae for the production of biodiesel. *Journal of Applied Phycology* **21**, 559–567. https://doi.org/10.1007/s10811-008-9391-8.

Lee, C. S., Robinson, J. & Chong, M. F. 2014 A review on application of flocculants in wastewater treatment. *Process Safety and Environmental Protection* **92**, 489–508. https://dx.doi.org/10.1016/j.psep.2014.04.010.

Li, Z., Zhong, S., Lei, H. Y., Chen, R. W., Yu, Q. & Li, H. L. 2009 Production of a novel bioflocculant by *Bacillus licheniformis* X14 and its application to low temperature drinking water treatment. *Bioresource Technology* **100**(14), 3650–3656. https://doi.org/10.1016/j.biortech.2009.02.029.

Lian, B., Chen, Y., Zhao, J., Teng, H. H., Zhu, L. & Yuan, S. 2008 Microbial flocculation by *Bacillus mucilaginosus*: applications and mechanisms. *Bioresource Technology* **99**(11), 4825–4831. https://doi.org/10.1016/j.biortech.2007.09.045.

Liu, W., Wang, K., Li, B., Yuan, H. & Yang, J. 2010 Production and characterization of an intracellular bioflocculant by *Chryseobacterium daeguense* W6 cultured in low nutrition medium. *Bioresource Technology* **101**(3), 1044–1048. https://doi.org/10.1016/j.biortech.2009.08.108.

Liu, W., Cong, L., Yuan, H. & Yang, J. 2015 The mechanism of kaolin clay flocculation by a cation-independent bioflocculant produced by *Chryseobacterium daeguense* W6. *AIMS Environmental Science* **2**(2), 169–179. https://doi.org/10.3934/environsci.2015.2.169.

Ma, Q., Qu, Y., Shen, W., Zhang, Z., Wang, J., Liu, Z., Li, D., Li, H. & Zhou, J. 2015 Bacterial community compositions of coking wastewater treatment plants in steel industry revealed by illumina high-throughput sequencing. *Bioresource Technology* **179**, 436–443. https://doi.org/10.1016/j.biortech.2014.12.041.

Marbelia, L., Bilad, M. R. & Vankelecom, I. F. J. 2019 Gradual PVP leaching from PVDF/PVP blend membranes and its effects on membrane fouling in membrane bioreactors. *Separation and Purification Technology* **213**, 276–282. https://doi.org/10.1016/j.seppur.2018.12.045.

Prigent-Combaret, C., Brombacher, E., Vidal, O., Ambert, A., Lejeune, P., Landini, P. & Dorel, C. 2001 Complex regulatory network controls initial adhesion and biofilm formation in *Escherichia coli* via regulation of the *csgD* gene. *Journal of Bacteriology* **183**(24), 7213–7223. https://doi.org/10.1128/JB.183.24.7213-7223.2001.

Qin, L., Liu, Y. & Tay, J. H. 2004a Effect of settling time on aerobic granulation in sequencing batch reactor. *Biochemical Engineering Journal* **21**(1), 47–52. https://doi.org/10.1016/j.bej.2004.03.005.

Qin, L., Tay, J. H. & Liu, Y. 2004b Selection pressure is a driving force of aerobic granulation in sequencing batch reactors. *Process Biochemistry* **39**(5), 579–584. https://doi.org/10.1016/S0032-9592(03)00125-0.

Rebah, F. B., Mnif, W. & Siddeeg, S. M. 2018 Microbial flocculants as an alternative to synthetic polymers for wastewater treatment: a review. *Symmetry* **10**(11), 1–19. https://doi.org/10.3390/sym10110556.

Reinhold-Hurek, B., Hurek, T., Gillis, M., Hoste, B., Vancanneyt, M., Kersters, K. & De Ley, J. 1993 *Azoarcus* gen. nov., nitrogen-fixing Proteobacteria associated with roots of Kallar grass (*Leptochloa fusca* (L.) Kunth), and description of two species, *Azoarcus indigens* sp. nov. and *Azoarcus communis* sp. nov. *International Journal of Systematic Bacteriology* **43**(3), 574–584. https://doi.org/10.1099/00207713-43-3-574.

Retna Raj, C. & Ramaraj, R. 2001 Emission of Thioflavin T and its off–on control in polymer membranes. *Journal of Photochemistry and Photobiology A: Chemistry* **74**(6), 129–137. https://doi.org/10.1016/S1010-6030(03)00320-4.

Rosenberg, E., DeLong, E. F., Lory, S., Stackebrandt, E. & Thompson, F. 2014 *The Prokaryotes*, 4th edn. Springer, Berlin, Heidelberg. https://doi.org/10.1007/978-3-642-30197-1.

Sarang, M. C. & Nerurkar, A. S. 2020 Amyloid protein produced by *B. cereus* CR4 possesses bioflocculant activity and has potential application in microalgae harvest. *Biotechnology Letters* **42**(1), 79–91. https://doi.org/10.1007/s10529-019-02758-3.

Thomsen, T. R., Kong, Y. & Nielsen, P. H. 2007 Ecophysiology of abundant denitrifying bacteria in activated sludge. *FEMS Microbiology Ecology* **60**(3), 370–382. https://doi.org/10.1111/j.1574-6941.2007.00309.x.

Van den Broeck, R., Van Dierdonck, J., Caerts, B., Bisson, I., Kregersman, B., Nijskens, P., Dotremont, C., Van Impe, J. & Smets, I. 2010 The impact of deflocculation-reflocculation on fouling in membrane bioreactors. *Separation and Purification Technology* **71**(3), 279–284. https://doi.org/10.1016/j.seppur.2009.12.006.

Vidal, O., Longin, R., Prigent-Combaret, C., Dorel, C., Hooreman, M. & Lejeune, P. 1998 Isolation of an *Escherichia coli* K-12 mutant strain able to form biofilms on inert surfaces: involvement of a new *ompR* allele that increases curli expression. *Journal of Bacteriology* **180**(9), 2442–2449. https://doi.org/10.1128/jb.180.9.2442-2449.1998.

Wang, J., de Ridder, D., van der Wal, A. & Sutton, N. B. 2021 Harnessing biodegradation potential of rapid sand filtration for organic micropollutant removal from drinking water: a review. *Critical Reviews in Environmental Science and Technology* **51**(18), 2086–2118. https://doi.org/10.1080/10643389.2020.1771888.

Wilderer, P. A., Rubio, M. A. & Davids, L. 1991 Impact of the addition of pure cultures on the performance of mixed culture reactors. *Water Research* **25**(11), 1307–1313. https://doi.org/https://doi.org/10.1016/0043-1354(91)90108-3.

Xin, X., Lu, H., Yao, L., Leng, L. & Guan, L. 2017 Rapid formation of aerobic granular sludge and its mechanism in a continuous-flow bioreactor. *Applied Biochemistry and Biotechnology* **181**(1), 424–433. https://doi.org/10.1007/s12010-016-2221-6.

Zaman, S. B., Hussain, M. A., Nye, R., Mehta, V., Mamun, K. T. & Hossain, N. 2017 A review on antibiotic resistance: alarm bells are ringing. *Cureus* **9**(6). https://doi.org/10.7759/cureus.1403.

Zhang, Z., Schwartz, S., Wagner, L. & Miller, W. 2000 A greedy algorithm for aligning DNA sequences. *Journal of Computational Biology* **7**(1–2), 203–214. https://doi.org/10.1089/10665270050081478.

First received 14 March 2023; accepted in revised form 16 June 2023. Available online 4 July 2023